

Proceedings of The Institute of Acoustics

METALLIC GLASS AS A HYDROPHONE MATERIAL

P. Walmsley

DBE Technology Group plc, Eastern Road, Aldershot

ABSTRACT The basic properties of metallic glass materials are reviewed with emphasis on characteristics applicable to hydrophone design. These include annealing treatments, stress-magnetic effects and geometrical configurations. Magnetostrictive principles are also reviewed and a membrane hydrophone proposed and analysed. Measured results are presented but agreement is poor reflecting the difficulty in characterising the material properties.

1. Introduction

Metallic glasses are amorphous (non-crystalline) alloys in which very rapid cooling from the melt causes the material to solidify before crystallisation can take place. The alloys discussed in this paper are of the basic composition $T_{90}M_{10}$ where T represents one or more transition metals like Fe, Ni, Co and M represents metalloid elements such as B, Si, C, P and Al (1). Basic properties of these alloys include very high permeability ($\mu_r > 100000$), very low coercive force ($H_c \approx 0.3 \text{ A/m}$), high tensile strength, and potentially cheap production. The purpose of this paper is to review these properties and to investigate the use of metallic glass in hydrophone designs.

Amorphous materials can be produced by a number of methods which achieve the very rapid cooling rates ($\sim 10^5 \text{ }^\circ\text{C/s}$) necessary to avoid crystallization. The most popular technique is filamentary casting in which molten material is ejected through an orifice under gas pressure onto the cooled surface of a rotating drum. By this means, ribbons of width in the range 0.1-180mm, thickness 5-50 μm and many kilometers long can be produced at rates of up to 2km/min. However such ribbons tend to have a smooth and curved upper surface, a flat and dimpled lower surface and high internal stresses.

Applications of the ribbon fall into two main categories (2). The first is in power devices where losses can be reduced by up to 4-5 times over 1% grain oriented silicon iron. Secondly the excellent magnetic and mechanical properties make the material suitable as a general replacement for nickel-iron alloys with applications such as magnetic shields, electronic delay lines, recording heads, switches and stress transducers.

2. Properties of Metallic Glasses

2.1 Basic Properties

The basic properties of some commercial alloys from Vacuumschmelze and Allied Chemical are summarized in Table 1 (3,4,5). However actual results vary considerably as a function of magnetic bias field and frequency. The ribbons can generally be described as soft ferromagnetic materials with a low saturation flux density. They can be cut, punched, etched, soldered or spot welded and can be bent through radii of curvature as small as 1mm.

METALLIC GLASS AS A HYDROPHONE MATERIAL

2.2 Magnetisation and Magnetostriction

The magnetic and magnetostrictive properties of metallic glasses can all be described qualitatively by principles applicable to crystalline materials (1). The shape of the magnetisation curve is determined by the different anisotropies (or short range order) within the material of which strain-magnetostriction anisotropy is particularly important. In as cast ribbons domain studies show a complicated 'labyrinthine' structure which changes under the influence of strain and magnetic field. This implies substantial boundary displacement during magnetisation (see Ref. 6 for a complete discussion of ferromagnetic domains in crystalline solids).

Changes in the magnetic moment exert forces on the atomic structure to produce small dimensional changes. Volume magnetostriction is usually small in comparison to the Joule effect which describes the length change in the direction of magnetisation. The opposite process, the Villari effect, is a change in magnetisation with stress as shown by the set of hysteresis loops for Vitrovac 7505 in Figure 1. The stress therefore has the same aligning character as an external field (5) but is very difficult to quantify (see Ref. 7 for a discussion of crystalline materials and Ref. 8 for amorphous alloys).

Magnetostriction in amorphous alloys varies according to composition from around -12ppm for $\text{Fe}_{0.7}\text{Co}_{0.4}\text{Ni}_{0.5}\text{P}_{17.4}$ to around +31ppm for $\text{Fe}_{80}\text{B}_{20}$ (1). For transduction purposes, the materials with largest magnetostrains are most sensitive and correlate well with iron content. Discussion in the remainder of this paper is therefore limited to materials such as Vitrovac 7505 ($\text{Fe}_{81}\text{B}_{13}\text{Si}_4\text{C}_2$), Metglas 2605SC ($\text{Fe}_{81}\text{B}_{13.5}\text{Si}_{1.5}\text{C}_2$) and Metglas 2605 ($\text{Fe}_{80}\text{B}_{20}$).

2.3 Variation in Properties with Annealing and Stress

Remarkable improvements in the magnetic properties of metallic glasses can be achieved by heat treatment. Much of this improvement can be attributed to the relief of internal strains introduced in the casting process and generally results in a lower coercive field, increase in remanent to saturation magnetisation ratio, increase in permeability and lower losses.

The annealing temperature is limited by the onset of crystallisation which in turn is a function of both temperature and time (see Ref. 1, p.478). Further improvement is obtained by annealing in a magnetic bias field at or above the Curie temperature so that stress relief precedes magnetic anneal (9). However even small amounts of crystallisation degrade transducer performance as shown by the variation of coupling coefficient with anneal temperature in Figure 2 (from Ref. 10). After anneal, the complex domain structure disappears leaving only a few domain walls and a magnetisation process that is predominantly rotational (11).

Change in magnetic properties by strain-magnetostriction anisotropy is also sensitive to sample geometry. Luborsky and Becker (12) have found that the properties of ribbon wound toroids vary with toroid diameter, winding tension, ribbon width and also number of laminations and direction of winding. This is due to both compression and tension caused by bending stresses, ribbon toroids showing predominantly compressive behaviour. Generally compressive stress in a positive magnetostriction material acts to increase the coercive force, decrease the remanent to saturation magnetisation ratio and decrease the permeability in the as cast state (13). However Poisson's ratio effects and internal stresses from the quenching process all interfere to complicate the final stress distribution.

Metallic glass toroids also show large effects due to leakage flux (see Ref. 14 for a discussion of leakage flux in thin magnetic materials). This is shown in Figure 3 where the flux detected around 10 layer toroids (Vitrovac

METALLIC GLASS AS A HYDROPHONE MATERIAL

7505, 25 μ m thick, 10mm wide) of 40-100mm diameter varies as a function of pick-up coil position relative to a small drive coil, each coil of length 15mm. Detected flux was also found to vary with number of layers but surprisingly not with pick-up coil diameters up to 42mm.

3. Magnetostrictive Hydrophones

3.1 Theory

A polarised (magnetically biased) magnetostrictive material exhibits linear piezomagnetic action under small signal excitation for which the following pair of equations is valid (15).

$$S_3 = s_{33}^H T_3 + d_{33} H_3 \quad (1)$$

$$B_3 = d_{33} T_3 + \mu_{33}^I H_3 \quad (2)$$

where H_3 is the magnetic field in the biased direction (in this case the long axis of the ribbon) and T_3 is the stress in this direction which produces a strain S_3 and flux density B_3 . The piezomagnetic constant d_{33} , the elastic compliance s_{33}^H at constant H or B and the permeability at constant stress μ_{33}^I are defined as the partial derivatives of S , H , B and T from equations 1 and 2.

The magnetoelastic coupling coefficient describing the basic energy conversion capability of the material is given by

$$k_{33}^2 = d_{33}^2 / \mu_{33}^I s_{33}^H \quad (3)$$

$$\text{and} \quad s_{33}^B = s_{33}^H (1 - k_{33}^2) \quad (4)$$

3.2 Piezomagnetic Constants for Metallic Glass

The results of measurements by Brouha and van der Borst (16) are shown in Figures 4-6 for as quenched $\text{Fe}_{80}\text{B}_{15}\text{Si}_5$ ribbon and material annealed for 30 minutes at 300 °C under different bias field orientations. Similar results have been obtained by the author for as quenched Vitrovac 7505. Meeks and Clifton Hill (17) have obtained even better results by optimally annealing Metglas 2605SC for 10 minutes at 369 °C in a transverse magnetic field of 0.4 MA/m. They achieve a maximum coupling coefficient of 0.9 and a d_{33} coefficient of almost 400 nWb/N. This coefficient is about 50 times larger than that of nickel. Further they report a figure of merit, as defined by Woollett (18) to reflect the sensitivity and impedance of a sensor material, of $g_{33} d_{33} = d_{33}^2 / \mu_{33}^I = 325 \times 10^{-13} \text{ m}^2/\text{N}$ for one sample. This compares with a figure of merit for ceramic (PZT4) of around $72 \times 10^{-13} \text{ m}^2/\text{N}$. On this basis, metallic glass is 4.5 times a better sensor than ceramic.

3.3 Equivalent Circuit

The equivalent circuit representing an acoustically small magnetic field hydrophone with a single dominant resonance is shown in Figure 7. This circuit is the current analogue of an electric field device and possesses the dual receiving characteristics shown in Figure 8. For the flat, low frequency current response region, the circuit reduces principally to inductive components for which the coupling coefficient can be written

Proceedings of The Institute of Acoustics

METALLIC GLASS AS A HYDROPHONE MATERIAL

$$k^2 = L_2 / (L_1 + L_2) \quad (5)$$

The free field voltage and current sensitivities are

$$M_0 = \omega L_2 A / \alpha \quad (6)$$

$$M_s = M_0 / (R_s^2 + \omega^2 (L_1 + L_2)^2)^{1/2} \quad (7)$$

where A is the active area of the device, α is the electromechanical transformation ratio and ω is the angular frequency. L_1 and α are not usually evaluated explicitly but are combined in the piezoelectric coefficient and relationship between acoustic pressure and stress in the material.

Perhaps due to the difficulty in characterising metallic glass, very few practical sensors have been reported. Mohri et al (19,20) have described two types of force or shock transducers using both toroidal cores and a stretched ribbon. Savage and Spano (11) have described a strain gauge or hydrophone operating by deflection of a composite beam and also derive expressions for a hydrostatic version of this configuration. High hydrostatic figures of merit ($g.d = 1 \times 10^{-12} \text{ m}^2/\text{N}$) are claimed for this mode without the use of pressure release materials. Indeed the nature of the ribbon allows it to be stretched around a variety of formers and the performance of a membrane device will now be described.

4. Performance of a Magnetostrictive Membrane Hydrophone

4.1 Construction

In general, beam or membrane designs are the best transformers of applied stress to longitudinal strain compared with hydrostatic modes or cylindrical tubes etc. of a similar size. For this reason, the membrane design shown in Figure 9 was chosen. The transducer consists of two UPVC (low permeability) blocks into which a rectangular recess measuring $30\text{mm} \times 12.5\text{mm} \times 3\text{mm}$ deep was cut. Each recess was covered and sealed with a single layer of cling film. 10 layers of 'as cast' Vitrovac 7505 ribbon, each layer measuring approximately $80\text{mm} \times 10\text{mm} \times 25\mu\text{m}$ thick were placed on top of the cling film and clamped at each end of the recess. The whole section between the clamps was then encapsulated in polyurethane to a depth of around 2mm sealing the ribbon over the air gap with minimal restriction to deflection.

Around the ribbon and air gap of each block, 500 turns of wire were wound as a pick-up coil and 25 turns as a polarising coil. The two halves were then placed back-to-back with the coils connected to cancel voltages produced by external magnetic fields. Finally the whole device was placed inside an oil-filled rubber boot containing an electrical gauze screen. The boot was sealed by a screw top with 'O' rings.

4.2 Analysis

Analysis of the transducer proceeds as for a one dimensional tension controlled (low frequency) membrane under free field and uniform pressure conditions. Restoring forces on the underside of the membrane due to compression of air in the recess and flexural rigidity are assumed negligible. Both assumptions have been theoretically verified.

The analysis follows the energy method described by Timoshenko and

METALLIC GLASS AS A HYDROPHONE MATERIAL

Woinowsky-Krieger (21) in which strain is assumed uniform across the membrane. For a membrane of length $2a$, thickness h and Young's modulus E we obtain the tension in response to a pressure P on one surface as

$$T = (4/\pi^2)^{1/3} \sqrt{P^2 a^2 E/h^2} \quad (8)$$

Linearising equation 8 for a small signal pressure, the change in flux density for constant external magnetic field is given by equation 2. Hence the voltage generated across a coil of N turns gives the open circuit voltage sensitivity

$$M_0 = 0.365 N b h d_{33} \omega \sqrt{\frac{a^2 E^4}{h^2 P_0}} \quad (9)$$

where b is the ribbon width and P_0 is the hydrostatic pressure. The fundamental frequency of flexural resonance is given as for a flexible string

$$f = 1/4a \sqrt{T/\sigma} \quad (10)$$

where σ is the mass per unit area of the membrane.

4.3 Results and Discussion

The measured free field voltage and current sensitivities at a polarising current of 1A are shown in Figure 10 and the change in sensitivity with polarising current is shown in Figure 11. The main feature of Figure 10 is a large antiresonance at 62.5kHz in both the current and voltage sensitivities. This cannot be easily explained but a likely cause is phase interference in the device structure. Also visible is the approach of resonance below 10kHz (where measurements became difficult in the tank used), an electrical resonance in M_0 at 30kHz and a general $1/\omega$ fall-off in response between 20kHz and 120kHz. Unfortunately with the ribbon clamped at both ends, impedance loop measurements show only electrical behaviour in this device.

In Figure 10, the low frequency voltage sensitivity is estimated from the height of the resonance peak ($\approx 20 \log_{10} Q$) to be around -215dB re 1V/ μ Pa at 10kHz. Using dimensions given in section 4.1 and a static pressure of 10 kPa (1m depth) equation 9 gives a value for d_{33} of 8.19×10^{-11} Wb/N. Compared with the results of Brouha (Figure 6), this figure is low by about 3 orders of magnitude for the as quenched material. A static pressure test on the ribbon with an integrating flux meter gave an effective d_{33} constant of 1.05×10^{-9} Wb/N. In turn this is around a factor of 8 worse than the values calculated from the static curves for a straight ribbon in Figure 2.

Polar plots at 100kHz, where beamwidths should nominally be 30° and 90° in the two orthogonal planes are shown in Figure 12. These indicate that behaviour is far from ideal and we can only conclude that poor device performance is a combination of frequency and geometry effects such as leakage flux and unequal tension in all ribbon layers.

Comparison of this device with a ceramic membrane is inappropriate due to the difficulty in fabrication of a thin ceramic. However a PVDF element could be made in similar dimensions and application of equation 9 gives a theoretical sensitivity $M_0 = -155$ dB re 1V/ μ Pa for such a device. By comparison, the optimum d_{33} values reported by Meeks for Metglas 2605SC (Ref. 17) should give an M_0 value of -145dB re 1V/ μ Pa at 10kHz!

METALLIC GLASS AS A HYDROPHONE MATERIAL

5. Conclusions

Metallic glasses with high iron content are potentially very cheap magnetostrictive materials with excellent mechanical and soft magnetic properties. Magnetostrictive properties are greatly improved by annealing in a transverse magnetic field and although heat treatment embrittles the material values of coupling coefficient higher than 0.9 can be achieved. Optimally annealed ribbons are 50 times more stress sensitive than traditional nickel and possess a figure of merit 4.5 times greater than PZT4 ceramic. However absolute performance is very difficult to predict due to variation in properties with stress, magnetic field and effects of leakage flux.

Magnetostrictive hydrophones are current analogues of electric field devices and in comparison are generally more robust with low output impedance. The principal advantage of a metallic glass hydrophone is high potential sensitivity where its characteristics are suitable for driving long lengths of cable without a preamplifier. Design configurations are flexible but further work is necessary to achieve a useful device.

6. Acknowledgements

The author would like to thank the directors of DBE Technology Group plc for financial support and facilities and also the MoD under whose contract this work was performed together with the SERC and the University of Bradford. Thanks are equally due to Mr. E. Rolfe of Rolfe Industries for the provision of Vitrovac metallic glass samples.

7. References

1. F.E. Luborsky, in *Ferromagnetic Materials Vol. 1*, (Ed. E.P. Wohlfarth), North Holland Publishing Co., (1980), Ch. 6.
2. K.J. Overshott, *Electronics and Power*, (May 1979), pp 347-350.
3. Vacuumschmelze GmbH, Vitrovac Brochure, Hanau Works, Grüner Weg 37, D-6450 Hanau 1, W. Germany, (1983).
4. Allied Corporation, Metglas Brochure, 6 Eastmans Road, Parsippany, New Jersey 07054, USA, (1981).
5. R. Grössinger et al, *Z. Metallkunde*, Bd. 74, (1983), H.9, pp 577-584.
6. C. Kittel, *Rev. Mod. Phys.*, 21, 4, (1949), pp541-583.
7. F. Brailsford, *Physical Principles of Magnetism*, Van Nostrand, (1966), Ch.6
8. H.R. Hilzinger et al, *Phys. Stat. Sol. (a)*, 55, (1979), pp 763-769.
9. L.T. Kabacoff, *J. Appl. Phys.*, 53, 11, (1982), pp 8098-8100.
10. M.A. Mitchell et al, *IEEE Trans. MAG-14*, 6, (1978), pp 1169-1171.
11. H.T. Savage, M.L. Spano, *J. Appl. Phys.*, 53, 11, (1982), pp 8092-8097.
12. F.E. Luborsky, J.J. Becker, *IEEE Trans. MAG-15*, 6, (1979), pp 1939-1945.
13. L. Lanotte, *J. Physique - Lettres*, 44, (1983), pp L541-L546.
14. H.J. Oguey, *Rev. Sci. Instrum.*, 31, 7, (1960), pp 701-709.
15. D.A. Berlincourt et al, in *Physical Acoustics*, (Ed. W.P. Mason), Academic Press, New York, (1964), Vol. 1, Part A, Ch. 3.
16. M. Brouha, J. van der Borsc, *J. Appl. Phys.*, 50, 11, (1979), pp 7594-7596.
17. S.W. Meeks, J. Clifton Hill, *J. Appl. Phys.*, 54, 11, (1983), pp 6584-6593.
18. R.S. Woollett, *J. Acoust. Soc. Am.*, 34, (1962), p. 522.
19. K. Mohri, E. Sudoh, *IEEE Trans MAG-15*, 5, (1979), pp 1806-1808.
20. K. Mohri, S. Takeuchi, *IEEE Trans MAG-17*, 6, (1980), pp 3379-3381.
21. S.P. Timoshenko, S. Woinowsky-Krieger, *Theory of Plates and Shells*, Mc Graw Hill, (1970), Ch. 13.

TABLES AND FIGURES

PROPERTIES	SYMBOL UNITS	VITROVAC			METGLAS		
		7505	4040	6025	2626	2605	2615
Composition		$\text{Fe}_{81}\text{B}_{12}\text{Si}_4\text{C}_2$	$\text{Fe}_{39}\text{Ni}_{39}\text{Mo}_2\text{Sn}_6\text{B}_{12}$	$\text{Co}_{36}\text{Fe}_{14}(\text{MoSiB})_{30}$	$\text{Fe}_{40}\text{Ni}_{20}\text{P}_{10}\text{B}_5$	$\text{Fe}_{90}\text{B}_{10}$	$\text{Fe}_{90}\text{P}_{10}\text{C}_2\text{B}_1$
Sat ⁿ Flux Density	$B_s(\text{T})$	1.50	0.80	0.55	0.87	1.60	1.48
Remanence/Sat ⁿ	$B_r/B_s(\text{T})$	0.8-0.9	0.8-0.9	0.8-0.9	0.45	0.51	0.40
Coercive Field	$H_c(\text{A/m})$	<4	<1	<0.4		~15typ	
Curie Temp.	$T_c(\text{K})$	693	533	523	520	647	565
Sat ⁿ Magnetost ⁿ	$\lambda_s(10^{-6})$	30	8	0.5	11	31	29
Density	$\rho(\text{kg/m}^3)$	7100	7400	7700	7500	7400	7700
Young's Modulus	$E(\text{GPa})$	150	150	150	147	172	138
Stack Factor		>0.8	>0.8	>0.8		>0.75	
Resistivity	$\rho(10^{-8}\Omega\text{m})$	130	135	135		130	
Tensile strength	$\sigma_T(\text{GPa})$		1.5-2.0	1.5-2.0			

TABLE 1 Typical Properties of Selected Amorphous Alloys (as cast)

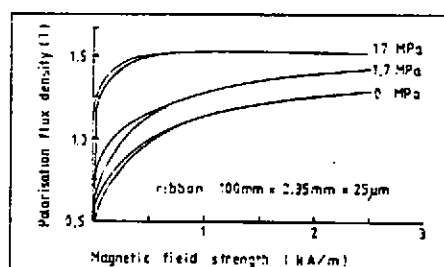


Figure 1 J-H loops under stress

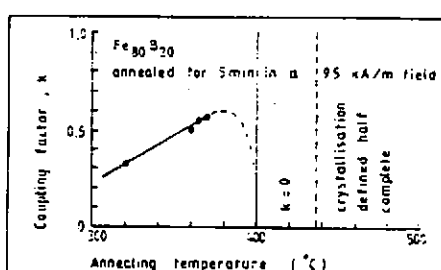


Figure 2 Annealing effect on k (Ref. 12)

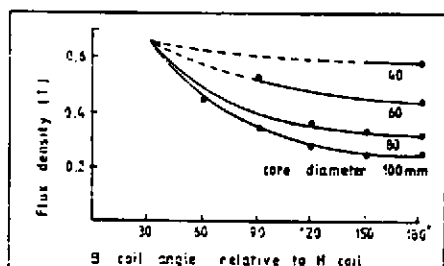


Figure 3 Toroid flux from local field

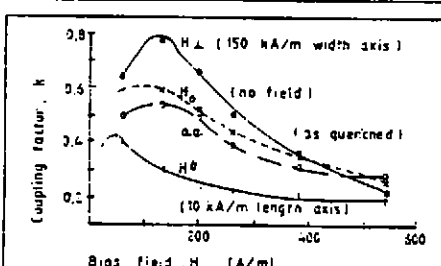


Figure 4 k-factor v. H-field (Ref. 16)

METALLIC GLASS AS A HYDROPHONE MATERIAL

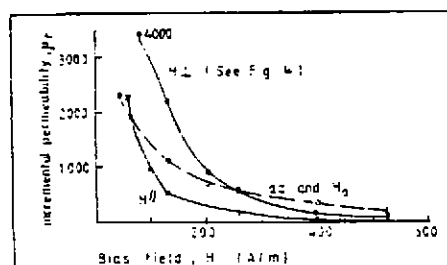


Figure 5 Permeability μ_r H-Field (Ref.16)

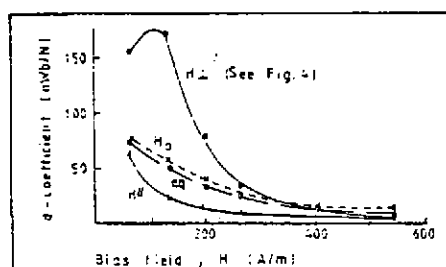


Figure 6 d-coefficient v. H-Field (Ref.16)

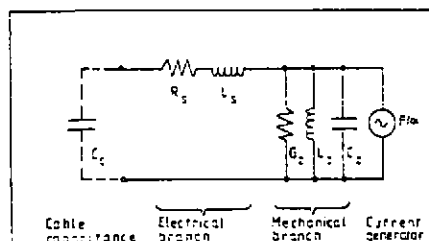


Figure 7 Magnetic field hydrophone

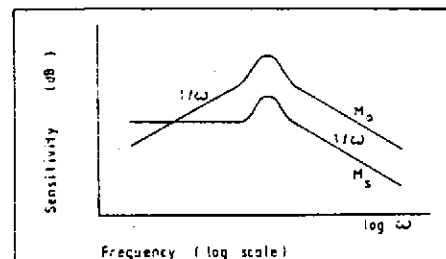


Figure 8 Magnetic field RX responses

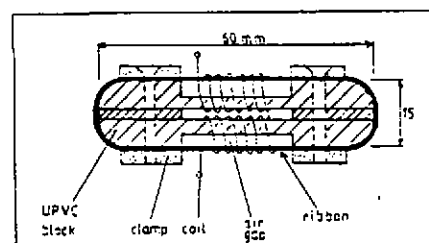


Figure 9 Membrane hydrophone section

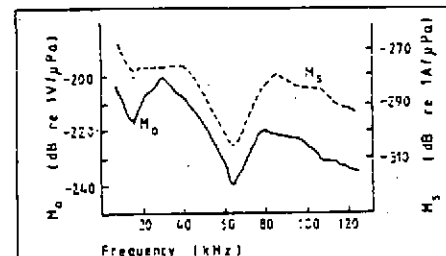


Figure 10 Membrane hydrophone response

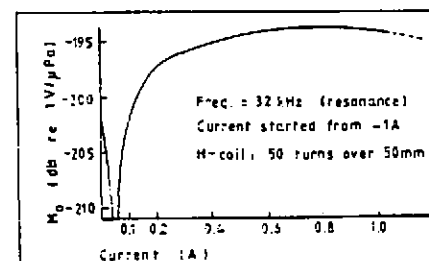


Figure 11 Sensitivity μ_r polarising current

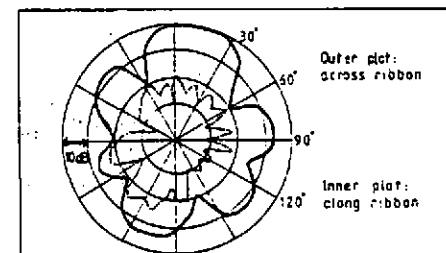


Figure 12 Polar plots at 100kHz